SPECTRAL MEASUREMENT AND ANALYSIS OF SILICON CMOS LIGHT SOURCES

A.W. Bogalecki*, M. du Plessis**, P.J. Venter** and C. Janse van Rensburg*

* *INSiAVA (Pty) Ltd, P. O. Box 14679, Hatfield, Pretoria, 0028, South Africa*
** *Carl and Emily Fuchs Institute for Microelectronics, Dept. of Electrical, Electronic & Computer Engineering, Corner of University Road and Lynnwood Road, University of Pretoria, Pretoria 0002, South Africa. E-mail: alfons.bogalecki@gmail.com*

Abstract: The emission spectra of *pn*-junction and punch-through (PT) carrier injection silicon (Si) CMOS light sources were measured at various current densities and temperatures. In contrast to the narrow-band forward-biased junction spectrum, that peaks around 1.1 μm (1.1 eV), the reverse-bias spectrum was found to extend from about 350 nm (3.4 eV) to about 1.7 μm (0.7 eV) covering the UV, Vis and NIR regions. Since the photon energy decreases with increasing wavelength, the significant NIR radiation implies that the quantum conversion efficiency of Si avalanche light sources is appreciably higher than previously reported. Calculating the photon flux at the emission source within the Si against photon energy allowed the deduction and quantification of the physical light emission processes with respect to silicon's electronic band structure. Intra-conduction-band (c-c) electron (e^-) transitions seem to be the dominant physical mechanism responsible for the wide avalanche spectrum.

Key words: Avalanche, CMOS, electroluminescence, light source, photon emission, silicon, spectrum, temperature

1. INTRODUCTION

1.1 Problem statement

Efficient on-chip Si light sources are desirable for wide-ranging applications that include optical data transmission, CMOS-integrated micro displays and micro-opto-electro-mechanical systems (MOEMS). Although Si electroluminescence (EL) was observed as early as 1955 [1], its high-speed capability [2] and long-term reliability [3] are established and the INSiAVA[1] group has improved the external power efficiency (EPE) of Si light sources by a factor 21 [4], relatively little is known about the physical EL processes and their dependence on factors such as current and temperature. In fact, there is still disagreement about the physical mechanisms responsible for the Si EL ([1], [3], [5] - [8]).

1.2 Background

While forward-biased Si *pn*-junctions are known to radiate strongly in a narrow band around 1.1 μm (1.12 eV), this light is due to the slow recombination of injected diffusing carriers, which limits the modulation speed of forward-biased *pn*-junction light sources to a few 100 kHz. For this reason, EL improvement research within the INSiAVA project focuses on wide-band, but fast-switching avalanching light source configurations that include *inter alia* reverse-biased *pn*-junctions and carrier-injection devices like punch- and reach-through ([9], [5]) Si light sources.

1.3 Approach

In this work, the EL spectra of two such Si light sources are investigated. Figure 1 shows the element layouts of the *pn*-junction and PT devices that were manufactured in 400 and 1760 element matrices respectively in the commercial austria micro systeme 0.35 μm four-metal CMOS process without any post-processing.
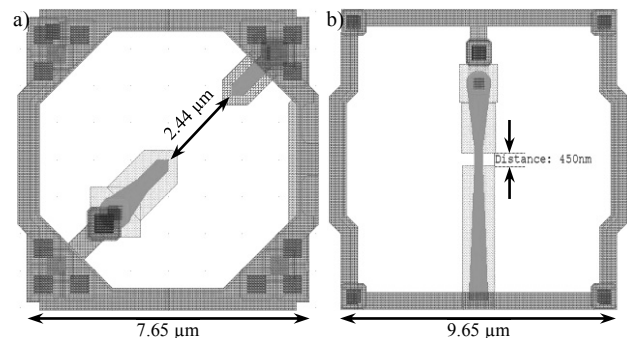

Figure 1: Element layouts of the a) n^+p-junction and b) n^+pn^+ PT CMOS light sources measured in this work.

The n^+ in *p*-substrate junction is pointed towards a p^+ substrate contact to increase the electric field and current density at the tip. The PT device consists of two n^+ diffusions that are spaced a specific distance from each other in the *p*-substrate so that PT carrier injection can occur [9]. The large open area around the light sources is necessary to prevent reflections or shielding from the surrounding metal interconnect layers.

These two CMOS light source matrices were measured at various device currents and temperatures with a Si UV-
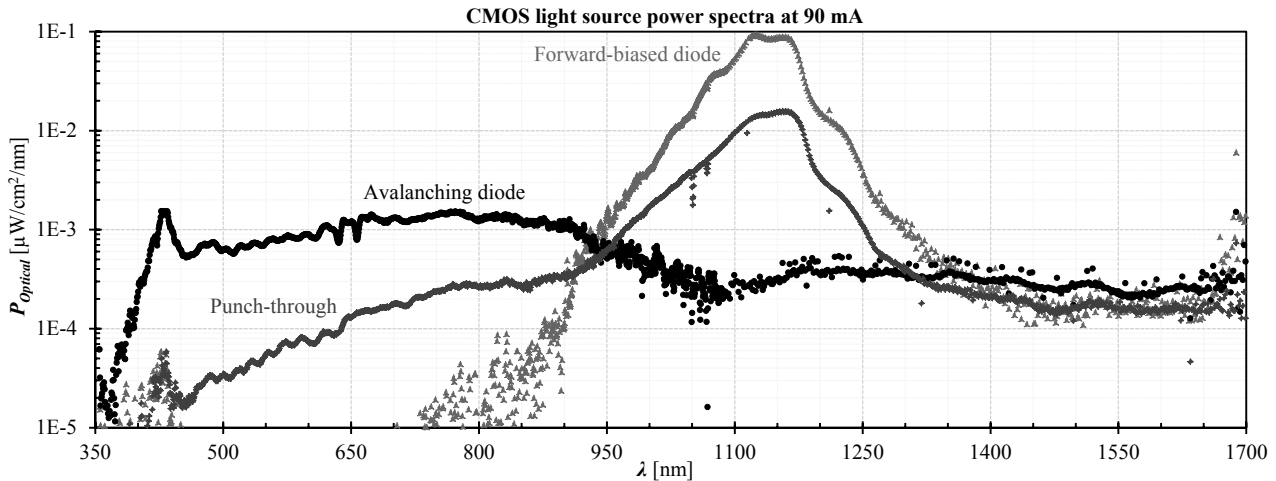
Figure 2: Spectrometer-measured power spectra of the avalanche, forward-biased and PT CMOS light sources.

Vis-NIR and an InGaAs NIR spectroradiometer that covered the wavelength ranges 177 nm – 1.1 μm and 894 – 1729 nm respectively. The two resultant spectra were then merged by taking into account the relative responses of the two spectroradiometers. By selectively filtering the spectroradiometer pixel noise and the wavelength-dependant Si-SiO$_2$-air stack interference and taking into account transmission losses through the Si-SiO$_2$-air stack, Si absorption and effective solid angles as seen by the spectroradiometers, the photon emission rates per photon energy at the light generation site were then calculated.

2.   MEASUREMENT RESULTS

2.1 Spectral Analysis

Figure 2 shows the typical external spectra of the avalanche, forward-biased and PT light sources measured at matrix currents of 90 mA. Although these measurements were measured at room temperature, the typical IC package temperature of the light source test-chips at such currents was about 31 ºC. The spectra in Figure 2 have not been filtered for noise or the wavelength-dependant Si-SiO$_2$-air stack interference and

clearly show the strong 1.13 μm peak of the forward-biased junction and weaker wide-band emission of the avalanching junction. The avalanche spectrum shows three distinct peaks: a narrow peak at 427 nm and two wide-tailed distributions around 761 nm and 1.25 μm. The PT light source combines attenuated spectra of both the forward-biased and avalanche light sources, but still has about twice the integrated optical power of the avalanche source.

A representative example of the resultant photon generation rates of the avalanche, forward-biased and PT CMOS light sources at room temperature are shown in Figure 3. These spectra experienced identical filtering and loss compensation and clearly show the 1.09 eV peaks of the forward-biased and PT sources. Avalanche peaks are visible around 0.9, 1.03, 1.41 and 2.89 eV.

Forward-bias and PT: The 1.09 eV peaks of the forward-biased and PT sources correspond to the shortest phonon-assisted (PA) conduction to valence (c-v) transitions in the energy bands of Si (Figure 4) and allow determining the temperature at the light generation site within the Si. At 300 K this band gap of Si is about 1.12 eV.
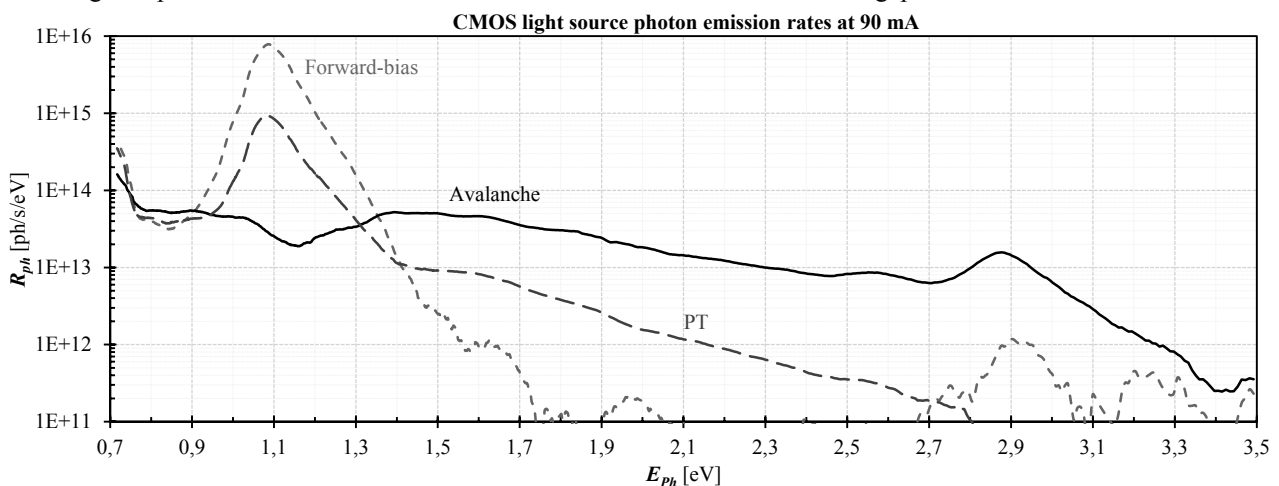

Figure 3: Calculated photon emission rate spectra of the avalanche, forward-biased and PT CMOS light sources.
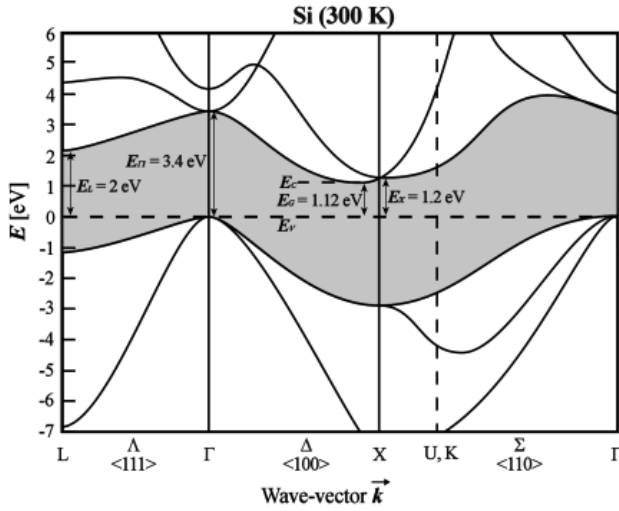
Figure 4: Si energy band diagram at 300 K [10].

The direct band gap energy of Si decreases with increasing temperature according to the experimentally determined relation ([10], pg. 15)

$$E_g(T) = E_g(0) - \frac{\alpha T^2}{T + \beta} \qquad (1)$$

where the fitting parameters have the values

$E_g(0)$= 1.1675 eV
α = 481.5 μeV/K
β = 645.5 K

According to (1) the temperature at the origin of the 1.1 eV peaks in the measured forward-biased and PT light sources was approximately 167 ºC.

Avalanche: Three possible radiative transitions might be responsible for the avalanche EL. Direct (non-PA) c-v transitions, which would show a emission peak at a photon energy of about 3.4 eV, PA c-v transitions, where emissions would peak around 1.12 eV plus the maximum of the e^- energy distribution in the conduction band, and c-c transitions, where the photon emission peak would coincide with the maximum e^- energy in the conduction band. One possible origin of the avalanche emission peak at 2.89 eV would therefore be direct (non-PA) c-v transitions. Considering that this gap requires an energy of about 3.4 eV at room temperature (Figure 4), the ΔE_{Ph} of at least 0.51 eV suggests a local temperature of about 1342 ºC, which seems impossibly high. If this mechanism is indeed responsible for the 2.89 eV avalanche emission peak, then raising the temperature of the device by 100 ºC should decrease the direct energy gap by about 40 meV. The temperature measurements in section 2.3 showed at most a shift of 7 meV, which seems to suggest that the spectral position of the 2.89 eV avalanche emission peak is independent of the temperature-variable band-gap and that this peak does not originate from direct c-v transitions.

Figure 5 shows simulated bulk e^- energy distributions in the conduction band for various electric field strengths. According to [11], the e^- distribution peak at 2.89 eV is due to the second maximum of density of states of electrons in the conduction band at this energy.
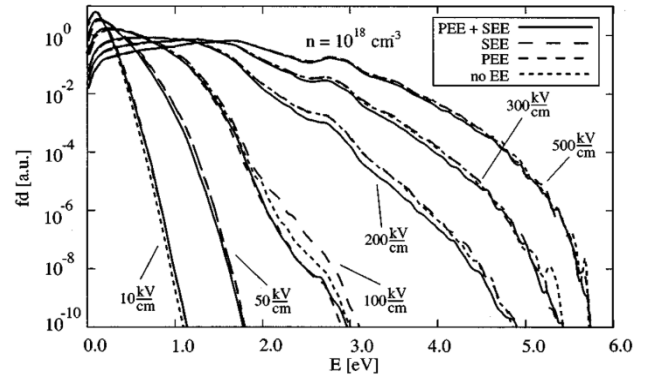

Figure 5: Electron energy distributions for different electric fields simulated by Mietzner *et al* [11].

The avalanche emission spectrum in Figure 3 with its 1.41 and 2.89 eV peaks and relative photon emission rate distribution for E_{Ph} > 1.17 eV agrees very well to a case where the electric field strength would be between 300 and 500 kV/cm. The measured breakdown voltage of about 9.8 V and estimated background doping of about $1.3 \cdot 10^{17}$ cm^{-3} suggests that the maximum electric field in the avalanche light source could reach strengths of up to 650 kV/cm. Although the magnitude of the electric field in the *pn*-junction device of Figure 1 is not yet known, the pointed n$^+$ diffusion is expected to increase the local electric field strength dramatically higher than 100 kV/cm. Since the n^+ diffusion is surrounded by the CMOS LOCOS field oxide, which through its curved "bird's beak" shape also shapes the diffusion vertically into a sharp tip, the electric field at the tip is enhanced even more.

Considering alternatively that the emission peak at 1.41 eV is due to hot e^- c-v transitions would imply an e^- distribution peak at 1.41 – 1.08 = 0.33 eV. Figure 5 consequently suggests an electric field strength of about 100 kV/cm, which seems too low for *pn*-junctions in reverse-bias avalanche breakdown.

The avalanche emission rate in Figure 3 drops by about 0.82 of an order of magnitude (factor 6.6) for an energy difference of about 1.05 eV between 1.41 and 2.46 eV. From Figure 5 a 400 kV/cm e^- energy distribution drops about by 0.85 of an order of magnitude (factor 7) from 1.5 eV to 2.5 eV. The 100 kV/cm distribution function drops from its peak at about 0.35 eV to 1.35 eV by more than two orders of magnitude (factor 110). The observation that the high energy tails of the avalanche emission agree very well with the e^- distribution function at about 400 kV/cm, but not at all at 100 kV/cm also reinforces the view that the avalanche emission is due to conduction to conduction (c-c) and not c-v transitions.

Similarly, the avalanche EL photon emission distributions around the peaks at about 0.91 eV, which has also been measured by *inter alia* [6] on NMOSFETs, and 1.02 eV can be explained as originating from direct inter-conduction band transitions in lower electric field regions along the flat edge of the n^+ diffusion and a distance away from the sharp diffusion corner. According to Figure 5 the average field strength away from the sharp corner is between 100 and 200 kV/cm.

The agreement between e^- energy distribution in Figure 5 and avalanche emission rate in Figure 3 seems to suggest that the electric field strength in the avalanche CMOS light source ranges between 100 kV/cm and about 400 kV/cm at the pointed diffusion corner. As also postulated by [6] and [8] the dominant avalanche light generation mechanism seems to be due to direct c-c e^- transitions.

2.2 Source current dependence

Figure 6 depicts the optical powers of the avalanche, forward-biased and PT CMOS light sources per µA integrated over the 350 – 990 nm and 990 – 1700 nm regions against varying source element current.
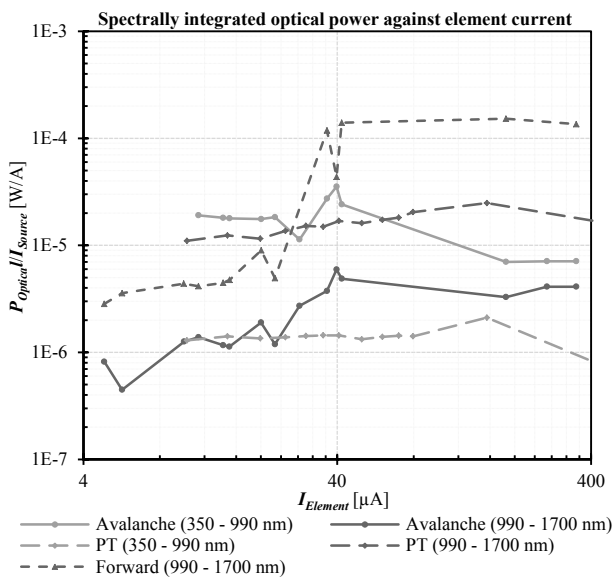

Figure 6: Measured integrated optical powers per source current against element current.

In effect, Figure 6 illustrates the effectiveness of each light source type in converting the current flowing through it into optical power. The overall trends are that the integrated optical power between 350 and 990 nm decreases with increasing source current, while the NIR radiation between 990 and 1700 nm increases with source current. The avalanche and forward-biased optical powers increase with source currents up to 40 µA after which the 350 - 900 nm radiation decreases with current while the 900 - 1700 nm optical remains relatively constant for driving currents above 40 µA/element. Although the exact reason for this phenomenon is still unknown, measurement error seems excludable as all three

independently measured data sets of the avalanching and forward-biased junction emissions show a similar maximum around 40 µA/element. The most probable reason for this behaviour is speculated to be the pointed diffusion shape of the diode CMOS light source in Figure 1 a). The 350 – 900 nm and 900 – 1700 nm PT power efficiency components as function of elemental source current exhibit similar trends with maxima around 156 µA/element.

Figure 7 shows the photon emission rate R_{Ph} per Source current I_{Source} of the avalanche CMOS light sources for four different source currents.
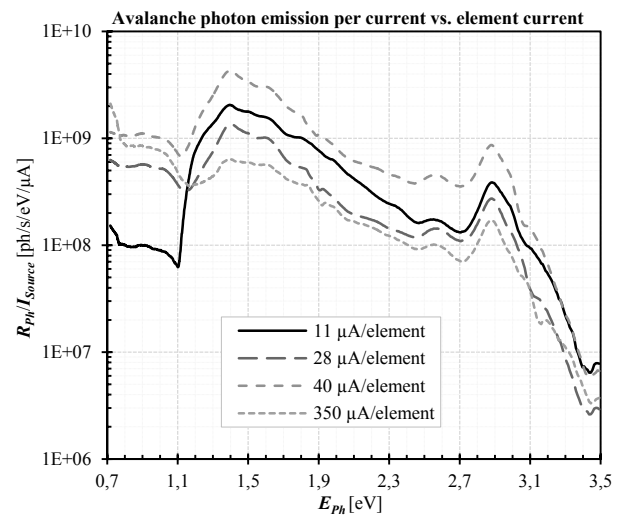

Figure 7: Measured avalanche photon emission rate R_{Ph} per source current for different source currents.

At low source currents, the avalanche light source is most efficient at emitting photons with energies between 1.17 eV and 3.2 eV with a peak at about 1.43 eV. As the source current increases, the photon emission rate above 1.17 eV decreases while photons with energies up to 1.17 eV are emitted at a growing rate. For element currents between 28 and 40 µA, photons above 1.17 eV experience an increasing emission rate. For $I_{Element} > 40$ µA the overall photon emission rate then decreases again, but this decrease is more pronounced for $E_{Ph} > 1.17$ eV.

One possible explanation for the decreasing R_{Ph} for $E_{Ph} > 1.17$ eV and increasing R_{PH} for $E_{Ph} < 1.17$ eV for $I_{Element} \leq 28$ µA is that for low currents the largest current flow and consequently largest e^- density occurs through the localized high electric field at the sharp tip of the n^+ diffusion. Forcing a higher device current increases the proportion of the current flowing across the flat diffusion edges on either side of the tip, which due to the lower electric field strength present there causes the increasing low-energy photon emission rate.

2.3 Temperature dependence

Avalanche: Figure 8 depicts the measured temperature dependence of the avalanche photon emission rate.
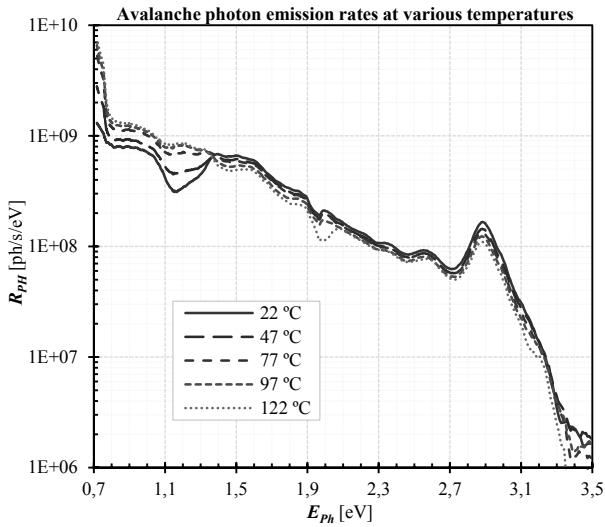
Figure 8: Measured avalanche photon emission rates for five selected IC package temperatures from 22 - 122 ℃.

As illustrated in Figure 9, after being almost equal at a temperature of 22 ℃, R_{Ph} increases almost linearly with temperature for $E_{Ph} < 1.37$ eV and fills the low-temperature dip at 1.18 eV in Figure 8, while the emission rate above 1.37 eV decreases with increasing temperature. At temperatures above about 100 ℃ the rate of increase with temperature of the 0.7 – 1.37 eV component and consequently the total photon emission rate slows down and flattens off.
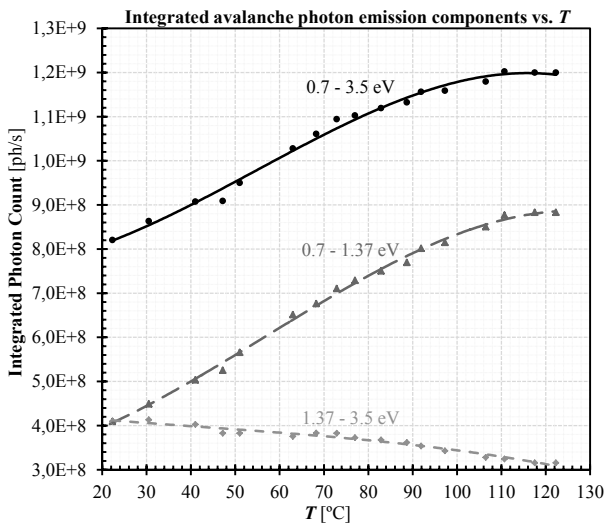

Figure 9: Integrated avalanche spectral components against temperature.

The negative temperature coefficient of $R_{Ph}(E_{Ph})$ for $E_{Ph} > 1.37$ eV was explained by [7] to be caused by factors such as decreasing impact ionization with increasing temperature. With increasing temperature, the avalanche multiplication rate decreases due to increased phonon scattering, which decreases the number of hot carriers travelling through the depletion region and consequently decreases radiative recombination. A secondary factor is

the increasing absorption of Si with increasing T. Although this theory explains the avalanche emission behaviour with temperature for $E_{Ph} > 1.37$ eV, it fails to explain the increasing EL with T for $E_{Ph} < 1.37$ eV.

Closer examination of the R_{Ph} peaks in Figure 8 reveals that neither of the peaks at 0.9 eV or 2.9 eV shift with temperature. Although it could also be an artefact of the changing R_{Ph} distribution around the peak at about 1.47 eV, it seems to be shifting by about 50 meV to higher photon energies when the temperature changes from 22 to 122 ℃.

Punch-through: Figure 10 shows the measured temperature dependence of the PT light source photon emission rate.
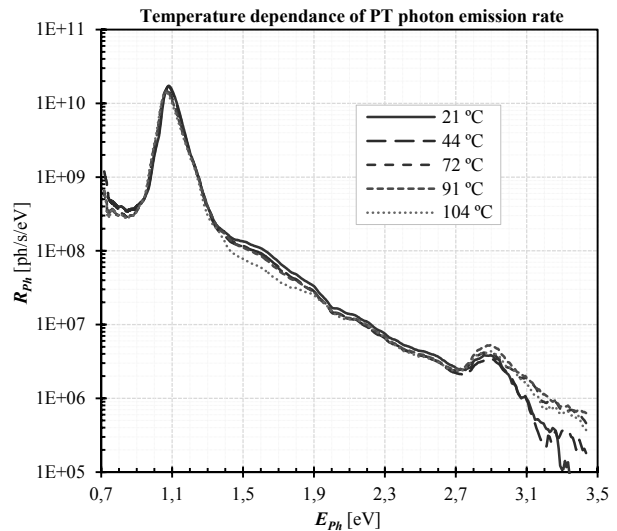

Figure 10: Measured PT photon emission rates for five selected IC package temperatures from 21 to 104 ℃.

The maximum of the PT emission spectra shifts from 1.093 eV at 21 ℃ to 1.089 eV at 104 ℃. According to (1) this shift of − 4 meV implies that the temperature at the site of light generation has increased from 110 ℃ to 163 ℃, a ΔT of 42 ℃ while the IC package temperature has increased by 83 ℃. The slight difference in temperature changes is attributed not only to unavoidable thermal gradients between the IC package and the light generation site, but also that longer temperature forcing settling periods and temperature measurements closer to the light generation site might be needed.

Although not measured, it is expected that the temperature behaviour of the 1.1 eV peak emission of the forward-biased *pn*-junction light source is similar to the abovementioned peak shift of the PT source.

Further investigation of Figure 10 reveals that while the PT photon emission rate falls with temperature for $E_{Ph} < 2.7$ eV, it increases above 2.7 eV. This behaviour is completely opposite to the avalanche emission temperature behaviour and currently unexplained.

3.   CONCLUSION

Spectroradiometric measurements of avalanching, forward-biased *pn*-junction and PT CMOS light sources in the wavelength range 350 – 1700 nm (0.7 – 3.5 eV) revealed their distinctly different photon emission spectra for different current densities and temperatures. While the forward-biased *pn*-junction showed the typical strong but narrow photon emission peak around 1.1 eV due to PA c-v carrier transitions, the wide-band avalanche spectrum seems to be mainly generated by direct hot e^- c-c transitions. The width and shape of the avalanche spectrum seems to relate to the electric field strength through which the electrons drift. Introducing high electric fields by utilizing sharp diffusion corners enhances the EL in the visible wavelengths dramatically. The PT light emission spectrum consists of a scaled combination of the forward-biased and avalanche spectra and while the spectral behaviour with current density is comparable to the respective dominant emission spectra of the forward-biased and avalanching *pn*-junction light sources, its temperature behaviour is distinctly different.

In general, the NIR emission for energies in the range 0.7 – 1.17 eV (1.1 – 1.7 μm) increases with increasing device current for all CMOS light sources. The photon emission in the energy range 1.25 – 3.5 eV (350 – 990 nm) of all CMOS light sources decreases with increasing current.

While NIR emission in the range 0.7 – 1.37 eV (0.9 – 1.7 μm) of the avalanche light source increases with temperature, photon emission in the energy range 1.37 – 3.5 eV (350 – 904 nm) decrease with increasing *T*. The temperature behaviour of the PT CMOS light source seems to be inverse to the avalanche source, but with a zero temperature coefficient near $E_{Ph} \approx 2.7$ eV (459 nm).

The overall result is that for visual display and Si detector applications, avalanching *pn*-junctions are the most efficient UV-Vis-NIR Si light sources and should be operated at low currents and temperatures. For applications where Si wave-guiding or long-wavelength detectors (like InGaAs) are desired, the PT and forward-biased Si light sources are superior and should be operated at high currents and low temperatures. The decisive difference between the PT and forward-biased light sources is that while the forward-biased source is an order of magnitude more efficient than the PT source, but the PT device is electrically modulateable above a few 100 kHz. Table 1 summarizes these recommendations with respect to Si light source requirements.

Table 1. Recommended Si CMOS light source parameters as a function of requirements.

Desired		Recommended			
		Type	Geometry	$I_{Element}$	T
UV-Vis-NIR	More UV-Vis	Avalanche	Sharp	Low	Low
	More NIR		Flat/Round	High	High
NIR	> 100 kHz, less effective	PT	Flat/Round	High	Low
	More effective, ≤ 100 kHz	Forward-bias			

4.   REFERENCES

[1] R. Newman, W.C. Dash, R.N. Hall and W.E. Burch: "Visible light from a Si p-n junction", *Phys. Rev.*, Vol. 98 A, pg. 1536, 1955.

[2] A. Chatterjee, B. Bhuva and R. Schrimpf: "High-speed light modulation in avalanche breakdown mode for Si diodes", *IEEE Electron Device Letters*, Vol. 25, No. 9, pg. 628, September 2004.

[3] A. Chatterjee and B. Bhuva: "Accelerated stressing and degradation mechanisms for Si-based photoemitters", *IEEE Transactions on Device and Materials Reliability*, Vol. 2, No. 3, pg. 60, 2002.

[4] A.W. Bogalecki and M. du Plessis: "Design and manufacture of quantum-confined punch through SOI light sources", *SPIE Photonics West symposium on Photonic Integration: Optoelectronic Integrated Circuits XII*, San Francisco, USA, pp. 76050B-1, January 2010.

[5] M. du Plessis, P.J. Venter and A.W. Bogalecki: "Using reach-through techniques to improve the external power efficiency of silicon CMOS light emitting devices", *SPIE Photonics West symposium on photonic integration: Silicon Photonics V*, San Francisco, USA, Paper 7606-37, January 2010.

[6] N.C. de Luna, M.F. Bailon and A.B. Tarun: "Analysis of near-IR photon emissions from 50-nm n- and p-channel Si MOSFETs", *IEEE Transactions on Electron Devices*, Vol. 52, No. 6, pp. 1211, 2005.

[7] M. Lahbabi, M. Jorio, A. Ahaitouf, M. Fliyou and E. Abarkan: "Temperature effect on electroluminescence spectra of silicon p–n junctions under avalanche breakdown condition", *Materials Science and Engineering*, Vol. B86, pp. 96–99, 2001.

[8] J. Bude: "Hot-carrier luminescence in Si", *Physical Review B*, Vol. 45, No. 11, pp. 5848, March 1992.

[9] P.J. Venter, M. du Plessis, M. Goosen, I.J. Nell and A.W. Bogalecki: "Improved efficiency of CMOS light emitters in punch-through with field oxide manipulation", *IEEE International Conference on Microelectronics 2010*, Cairo, Egypt, pg. 36, December 2010.

[10] S.M. SZE and K.K. Ng: *Physics of Semiconductor Devices*, Third Edition, John Wiley & Sons, Hoboken, New Jersey, 2007.

[11] T. Mietzner, J. Jakumeit, and U. Ravaioli: "Local iterative Monte Carlo analysis of electron–electron interaction in short-channel Si-MOSFETs", *IEEE Transactions on Electron Devices*, Vol. 48, No. 10, pg. 2326, October 2001.